

Model development for the conceptual design of a solar-powered aircraft air-conditioning system

Noah Sadaka ¹, Susan Liscouët-Hanke², Florian Sanchez ³

Concordia University, Montreal, Canada

One of the main goals of the aerospace industry is the reduction of the environmental footprint of aircraft. In this context, the introduction of an aircraft solar power system acting as an auxiliary electrical power source seems promising. In the next generation of aircraft, a solar power system could reduce fuel burn, noise, and improve passenger comfort and aircraft thermal management. In particular, a solar powered air-conditioning system seems promising. By use the solar energy, a fan or cooling system can avoid the heating up of the cabin and equipment bays for the aircraft parked on ground. In this way, the cooling energy required by the environmental control system can be reduced for the so-called pull-down operation and the reliability of electrical equipment can be improved. To estimate the potential benefits of such system, a modeling framework is established. This paper presents a parametric aircraft cabin transient thermal model developed to determine the reduction in required cooling power. A case study is presented for the Longview Aviation Q400⁴. The results show that enough power from the solar powered fan is available to keep the cabin and equipment bay at ambient temperature. This leads to a decrease in cooling load of up to 30%. Consequently, the reduction in required cooling load will require less powerful environmental control system and auxiliary power unit. The paper also addresses the impact on the sizing of the auxiliary power unit and environmental control system.

Keywords: *Aircraft solar power system, environmental control system, thermal modelling, conceptual aircraft design*

Introduction

The aerospace industry aims a significant reduction of its environmental footprint [1]. To achieve this goals, the development of new technologies is one promising avenue. In this context, the introduction of an aircraft solar power system (SPS) acting as an auxiliary electrical power source seems promising [2, 3, 4]. In the next generation of aircraft, an SPS could reduce fuel burn, noise, and improve passenger comfort & aircraft thermal management.

The prior work shows that an SPS could provide a significant amount of electrical power [4]. For example, the Q400, which with its high-wing and T-tail is the most promising aircraft configuration for an SPS, could have as much as 11.5 kW provided by the SPS on an average sunny day, which represents the power output of one of its engine-driven generators. This is important as it

¹Undergraduate student. Department of Mechanical, Industrial, and Aerospace Engineering. Email: noahsadaka@gmail.com

²Associate Professor. Department of Mechanical, Industrial, and Aerospace Engineering. Email: susan.liscouet-hanke@concordia.ca

³Post-Doctoral Researcher. Department of Mechanical, Industrial, and Aerospace Engineering. Email: florian.sanchez@mail.concordia.ca

⁴formerly Bombardier Aerospace

demonstrates that an SPS has the potential to shift the electricity production from combustion to photovoltaic, reducing fuel burn and generator weight. Work has also been done to integrate an SPS sizing tool into an aircraft multidisciplinary design workflow to show the potential benefit on an aircraft level [3, 5]. As part of a multi-disciplinary design challenge, an baseline aircraft was proposed for which an optimized aircraft design would need to be produced. This optimized aircraft was designed with an SPS, and had a reduced fuel weight and equivalent maximum take-off weight (MTOW) compared to the baseline aircraft.

Currently, aircraft are cooled on the ground using their environmental control system (ECS) which is provided bleed air from the auxiliary power unit (APU). As the APU is a gas turbine engine, it produces emissions and noise, and at hot airports is sometimes run continuously to keep the aircraft cool [6]. The aircraft can also be cooled using ground carts, however these are not available at all airports nor at all an airport's gates, especially for regional aircraft.

This paper presents a parametric, transient thermal model and applies this model for a case-study to estimate the potential size reduction of the APU and ECS due to the reduced cooling load it must provide during the so-called pull-down operation. This pull-down operation is the sizing case for the ECS [7], and is defined by the cooling energy required to reduce the cabin temperature of a heat-soaked aircraft on the ground to 28 degrees Celsius in 30 minutes. Since the ECS requires bleed air from the APU, the pull-down loading also sizes the bleed air required by the APU. By implementing a solar powered air conditioning system (SPACS), the pull-down loading is reduced and results in the resizing of the ECS and APU, aiding in offsetting the added weight of the SPS.

The proposed SPACS consist of fans which would reduce the rate at which the cabin and equipment bay heat up. The SPACS can increase aircraft independence by making airports in hot climates more accessible, particularly at those without ground carts. By reducing the reliance on the ECS and APU, emissions and noise pollution would be reduced.

Modeling Framework

To estimate the potential benefits of such a system, a modeling framework was established. Figure 1 shows the workflow, which required the creation of a cabin thermal model. This model calculates the pull-down loading for a conventional aircraft and for an aircraft with a SPACS to determine the

difference in pull-down. The APU size reduction is then determined. The reduction in size of the ECS is commensurate to the reduction of the required pull-down power.

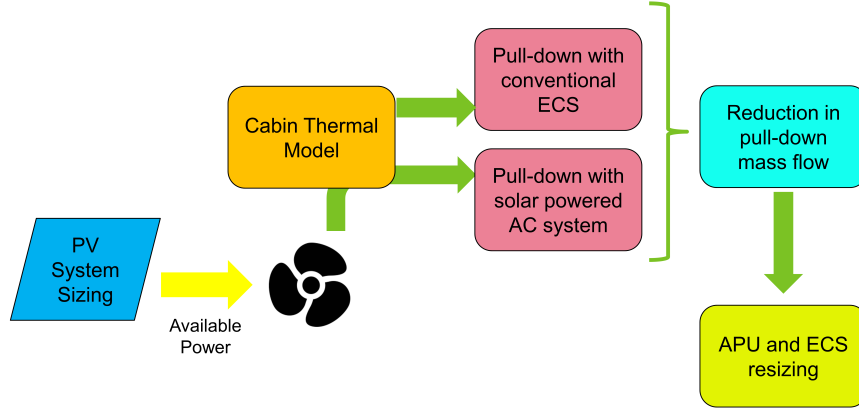


Figure 1: The modelling procedure.

Thermal Model

The thermal model is implemented using Modelica [8], a systems modeling language, and simulated using Dymola [9]. This model is a parametric 1D transient thermal model of an aircraft cabin. Different modes of heat transfer are considered in this model, as shown in Figure 2.

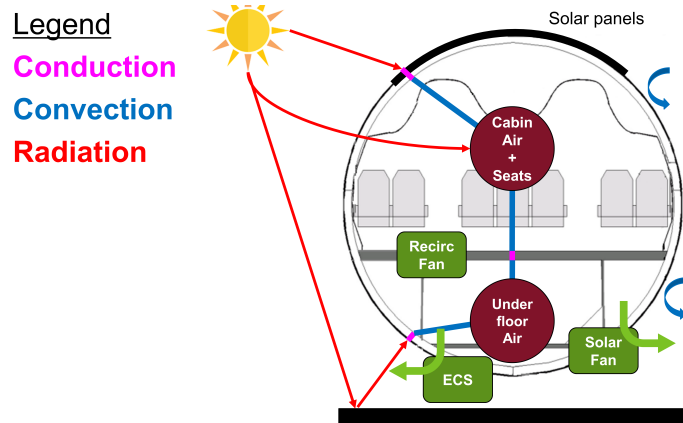


Figure 2: The different modes of heat transfer analyzed in the thermal model.

A lumped modeling approach was taken for the following elements: the fuselage wall layers, the cabin air and seats, and the underfloor. The fuselage wall is composed of an outer skin, followed by an insulation layer, an air gap, and an inner liner. The insulation layer is discretized into five sub-layers to achieve a smoother temperature distribution, which is necessary due to the insulation's

high thermal resistance. The cabin air and seats are combined into a single element, as there is no significant impact on cabin temperature if the seats are a separate element. The added mass of equipment in the underfloor is neglected.

In cases where the SPACS is present, the thermal effects of the solar panels are added to the fuselage. The solar panels are assumed to take up the top 136 degrees of the fuselage [4], and their heat conduction is assumed to be 30%, although this value is dependent on the materials used. Figure 3 shows an example of the the impact that the solar panel heat conduction has on cabin temperature.

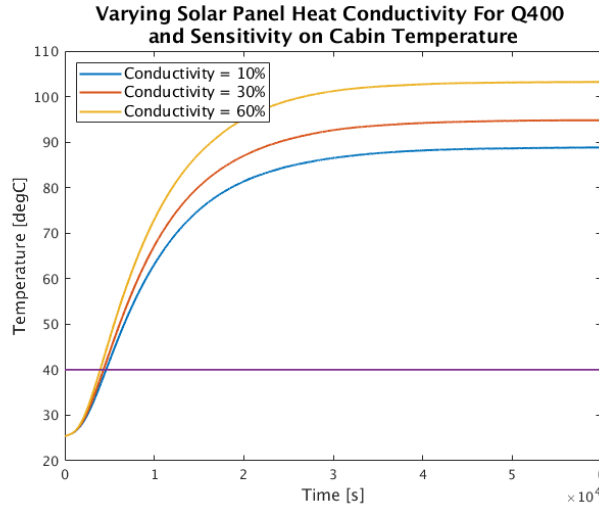


Figure 3: Impact of solar panel heat conduction on cabin temperature for the Q400.

The top half of the fuselage receives thermal energy through incident radiation from the sun, which is assumed to be at a 85 degree angle above the ground. Only direct radiation is considered, neglecting the diffusing effects of the atmosphere and clouds. The absorptivity of the fuselage is related to its color due to paint. The solar energy incident on the fuselage is calculated as:

$$\dot{Q}_{s,fus} = \alpha \cdot \dot{q}_{sol} \cdot R_{out} \cdot L \quad (1)$$

where

$$\begin{aligned} \alpha &= \text{Absorptivity of fuselage paint} \\ \dot{Q}_{s,fus} &= \text{Heat flow through the fuselage [W]} \\ \dot{q}_{sol} &= \text{Solar heat flux} = 950W/m^2 \\ R_{out} &= \text{Fuselage outer radius [m]} \\ L &= \text{Cabin length [m]} \end{aligned}$$

The bottom half of the fuselage receives radiation emitted by the tarmac below. A tarmac is typically made of a rigid pavement made of portland cement [10]. The albedo of this material ranges from 25% to 40%, darkening over time due to aircraft traffic. A value of 40% is used in the model to be conservative, and Equation 1 is multiplied by the albedo to give the radiative heat flux upon the bottom of the fuselage.

Solar radiation also enters the cabin through the windows. The amount of heat is calculated by [11]:

$$\dot{Q}_w = 0.5 \cdot \tau \cdot q_{sol} \cdot A_w \cdot \cos l \quad (2)$$

where

$$\begin{aligned} \dot{Q}_w &= \text{Heat flow through the windows [W]} \\ \tau &= \text{Window transmissivity} \\ A_w &= \text{Total area of the windows [m}^2\text{]} \\ l &= \text{Incidence angle between the Sun and the windows [deg]} \end{aligned}$$

Natural convection transfers heat between the upper and lower fuselage and the atmosphere. A heat transfer coefficient of $h = 8W/(K \cdot m^2)$ is used, which is a typical value used in industry for natural convection for a fuselage. The heat transfer due to natural convection is then calculated by [12]:

$$\dot{Q}_{nc} = h \cdot A \cdot (T_{fus} - T_{amb}) \quad (3)$$

where

$$\begin{aligned} \dot{Q}_{nc} &= \text{Heat due to natural convection [W]} \\ A &= \text{Fuselage area [m}^2\text{]} \\ T_{fus} &= \text{Skin temperature of the fuselage [K]} \\ T_{amb} &= \text{Ambient temperature [K]} \end{aligned}$$

The heat flow is calculated for both the upper and lower parts of the fuselage separately.

The heat flow is conducted through the different fuselage wall layers. Structural components that extend through these layers, such as frames and stringers, are not considered in this analysis. The conduction is modeled as an resistive-capacitive network, where the resistance is due to the thermal conductivity of each layer and the capacitance is due each layer's thermal mass. The thermal conductivity and specific heat capacity of each layer is provided in Table 1. The air gap is assumed to be thin enough to behave conductively.

Layer	Material	Thermal Conductivity $\left[\frac{W}{m^2 \cdot K}\right]$	Specific Heat Capacity $\left[\frac{J}{kg \cdot K}\right]$
Skin	Aluminum	155.76	921
Insulation	Glass fiber batting	0.035	1030
Air	Air	0.026	1003
Liner	Thermoset plastics	0.5	1900

Table 1: Resistive and capacitive material properties of the fuselage layers.

The temperature of a layer can be calculated by:

$$\frac{T_{i-1} - 2 \cdot T_i + T_{i+1}}{R} = c_p * m * \frac{dT_i}{dt} \quad (4)$$

where

T_i = The temperature at the layer i [K]

R = The resistance of the layer = $\Delta x / (k \cdot A)$ [K/W]

Δx = The layer thickness in the direction of heat flow [m]

k = The thermal conductivity $\left[\frac{W}{m^2 K}\right]$

A = The surface area normal to the direction of heat flow [m²]

c_p = The specific heat capacity $\left[\frac{J}{kg \cdot K}\right]$

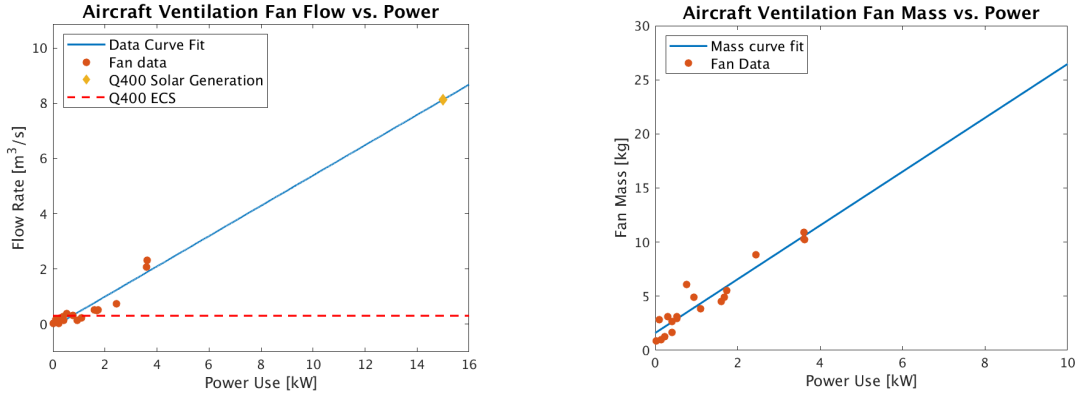
m = The layer mass [kg]

t = time [s]

Similarly, the heat flow across the floor layer is calculated using Equation 4. As the floor is assumed to be made of honeycomb core and thermoset resin sandwich panels, a thermal conductivity of $0.086 \frac{W}{m^2 \cdot K}$ and a specific heat capacity of $1900 \frac{J}{kg \cdot K}$ are used in Equation 4.

Natural convection is assumed for the heat transfer between the fuselage liner & floor and the cabin & underfloor. Equation 3 is used, but with a heat transfer coefficient $h = 5W/m^2K$ [13].

The solar-powered fan is modeled based on existing aircraft air circulation fans [14]. From a fan catalogue, the power required for a fan to produce a given mass flow was derived and is shown in Figure 4a. The weight of the fan can also be estimated based on Figure 4b.



(a) Relation between the fan flow and its power use.

(b) Relation between the fan mass and its power use.

Figure 4: Relations used to model the solar powered air circulation fan.

From Figure 4a, the following relation between fan power and air flow rate was created:

$$\dot{V}_{fan} = 0.0005482P_{fan} - 0.097675 \quad (5)$$

where

$$\begin{aligned} \dot{m}_{fan} &= \text{volumetric flow rate of air produced by the fan [m}^3\text{/s]} \\ P_{fan} &= \text{Power required by the fan [W]} \end{aligned}$$

The cooling capacity that the fan can provide is then calculated as:

$$\dot{Q}_{fan} = \dot{V}_{fan} \cdot \rho_{air} \cdot c_{p,air} \cdot (T_{uf} - T_{amb}) \quad (6)$$

where

$$\begin{aligned} \dot{Q}_{fan} &= \text{Heat flow out of the underfloor provided by the fan [W]} \\ \rho_{air} &= \text{Air density [kg/m}^3\text{]} \\ c_{p,air} &= \text{Air specific heat capacity } \left[\frac{J}{kgK} \right] \\ T_{uf} &= \text{Temperature of the underfloor [K]} \\ T_{amb} &= \text{Ambient temperature [K]} \end{aligned}$$

The environmental control system is modeled to determine the pull-down load. The mass flow of air is assumed to be based on CAR 525.831a [15], which requires 0.55 pounds per minute per passenger. The cooling load the ECS provides is calculated as:

$$\dot{Q}_{ECS} = \dot{m}_{ECS} \cdot c_{p,air} \cdot pax \cdot (T_{ECS} - T_{uf}) \quad (7)$$

where

$$\begin{aligned} \dot{Q}_{ECS} &= \text{Heat flow from the ECS [W]} \\ T_{uf} &= \text{Temperature of the underfloor [K]} \\ T_{ECS} &= \text{ECS outlet temperature [K]} \\ pax &= \text{Number of passengers} \\ \dot{m}_{ECS} &= \text{Mass flow of air from the ECS} = 0.55 \text{ lbs}/(\text{pax} \cdot \text{min}) \end{aligned}$$

Finally, a recirculation fan pulls air from the cabin to the underfloor when the solar fan or ECS are enabled. The recirculation fan is implemented as a component which transfers energy from the cabin to the underfloor according to:

$$\dot{Q}_{fan} = \dot{m}_{fan} \cdot c_{p,air} \cdot (T_{cab} - T_{uf}) \quad (8)$$

where

$$\begin{aligned} \dot{Q}_{fan} &= \text{Heat transferred from the cabin to underfloor [W]} \\ T_{cab} &= \text{Temperature of the cabin [K]} \\ \dot{m}_{fan} &= \text{Mass flow of air from the fan} = 1/3 \cdot \dot{m}_{ECS} \end{aligned}$$

Case Study: Q400

The developed thermal model is used for a case study for the Longview Aviation Q400. The Q400, as a regional aircraft with a high-wing and T-tail configuration is a promising candidate aircraft configuration for the potential implementation of an auxiliary solar power system.

The model variables specific to this case study are presented in Table 2.

Pull-Down Analysis

The above described thermal model is used to determine the pull-down time for various heat-soak durations. Figure 5 shows the cabin temperature variation for a conventional Q400 (no solar-powered fan), one with a 735W solar-powered fan, and one with a 5000W solar-powered fan. The 735W solar-powered fan has a mass flow of 0.383 kg/s, which is equal to that of the conventional Q400's ECS and would use existing fans and ducting to minimize on the weight impact and integration complexity. The 5000W solar-powered fan has a mass flow of 2.63 kg/s and would require the integration of a more complex system.

Variable	Symbol	Unit	Value
Ambient Temperature	T_{amb}	$^{\circ}\text{C}$	40
Skin thickness	Δx_{skin}	mm	1.2
Insulation thickness	Δx_{ins}	mm	76.2
Air gap thickness	Δx_{air}	mm	11.1
Liner thickness	Δx_{liner}	mm	1.5
Floor thickness	Δx_{floor}	mm	20
Passengers	pa_x	–	90
Fuselage outer radius	R_o	m	0.346
Cabin length	L	m	18.796
Number of underwing windows per side	–	–	3
Number of windows per side	N_w	–	26
Grey paint absorptivity	α	–	0.51

Table 2: Variables used in the thermal model for the Q400 case study.

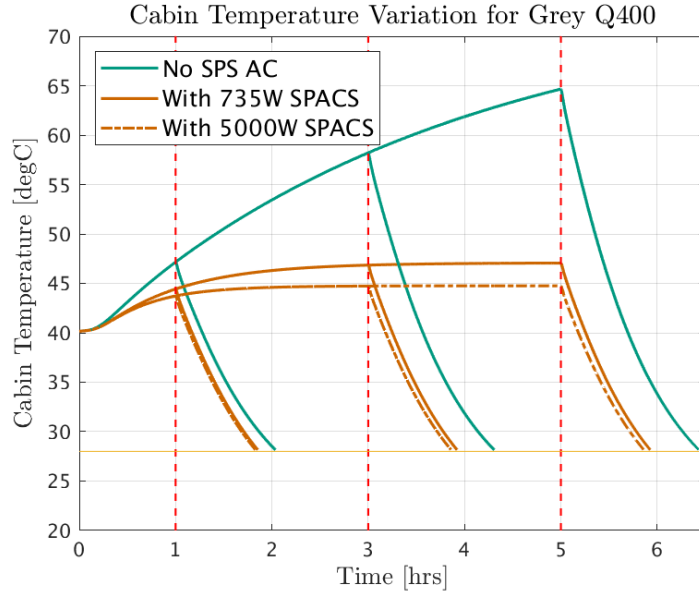


Figure 5: Pull-down results for a Q400 with a conventional ECS and with a solar powered air conditioning system. The pull-down is complete once the cabin temperature reaches 28° Celsius.

The ECS was turned on after at 1, 3, and 5 hours of heat soak. Compared to a conventional ECS, the SPACS allowed the cabin to reach a lower steady-state temperature in less time. A reduced pull-down time was achieved, as shown in Table 3, as was a corresponding reduced pull-down load. The 5000W solar-powered fan reduced the steady-state temperature more than the 735W solar-powered fan. However, a more powerful fan becomes limited by the heat transfer through the floor and the

amount of air transferred by the recirculation fan, resulting in diminishing returns for increased fan power.

Heat-soak time [hr]	Conventional ECS pull-down	735W SPACS pull-down	5000W SPACS pull-down
1	1.04	0.83	0.83
3	1.31	0.92	0.86
5	1.43	0.93	0.86

Table 3: Pull-down time for Q400 with conventional ECS and with a solar powered air conditioning system.

Based on this analysis, the potential effect on the ECS sizing was estimated. As shown above, the aircraft reaches an equilibrium temperature, and the ECS mass flow is adjusted to have the pull-down to 28 °C take 30 minutes. Table 4 shows that an aircraft with a 735W fan requires significantly less mass flow for the ECS to cool the cabin. This reduced mass flow allows the ECS and APU to be resized, which offsets the additional weight of the SPS and SPACS.

	ECS mass flow [kg/s]
Conventional ECS	0.71
735W SPACS	0.40
Percent Difference	55%

Table 4: Required ECS mass flow to reduce cabin temperature from heat-soaked to 28 °C in 30 minutes.

APU Sizing impact

From the reduced pull-down load with the SPACS, the potential reduced size of the APU is estimated. The assumption is made that the APU sizing case is the ECS pull-down. As the APU is also used for engine start, this case would need to be investigated in a more detailed study. As the ECS mass flow is provided by the APU load compressor while on ground, a relationship between the APU bleed air and the APU weight is analysed based on catalogue data [16, 17] and is shown in Figure 6.

Figure 6 shows significant spread in the data points. Maximum operable altitude, amount of electrical power generation, amount of bleed air production, and certification year all affect the weight. Here, the Pratt & Whitney Canada APS family of APUs is selected to show the relationship within the same APU family, as the technology within a single family is likely to be similar, removing

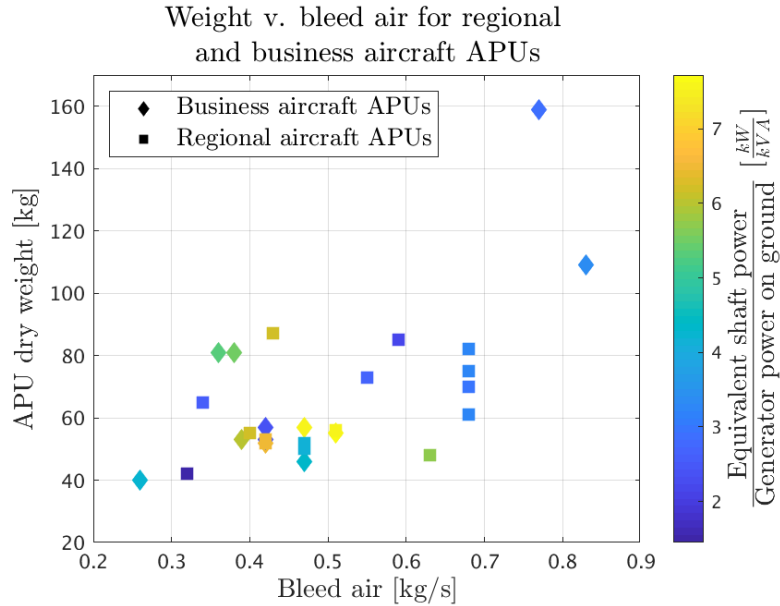


Figure 6: Relationship between bleed air production and APU mass.

a variable which impacts APU weight. The APU of the Q400, the APS1000, is a part of this family. Figure 7 shows the relationship between the bleed air production and the APU weight for the APS family of APUs.

Due to the influence on certification year on the APU weight, manifested by improvements in APU designs and technology for the same APU, clear trend can not be determined. However, upper and lower bands are added, the weight of the resized APU can potentially be reduced between 50-64% using a 735W SPACS. This shows that the potential weight is not negligible.

A relationship between mass flow and ECS weight was not determined due to a lack of publicly available data. However, the weight decrease due to the reduced pull-down loading would likely be proportional to that of the APU. Work is currently being done by other members of Dr. Liscouët-Hanke's research group to create a parametric ECS sizing model to link with the thermal model.

From Figure 4b and [5], the 735W SPACS would weigh around 5kg, although this value is optimistic as it does not consider the additional weight of power converters and other electrical components. The SPS (including solar panels of current technology, power converters and wiring) is assumed to be in the order of 10 kg for a 735W fan. Overall, considering the conceptual nature of this study and the associated uncertainties, the SPACS would potentially reduce the weight on an aircraft level.

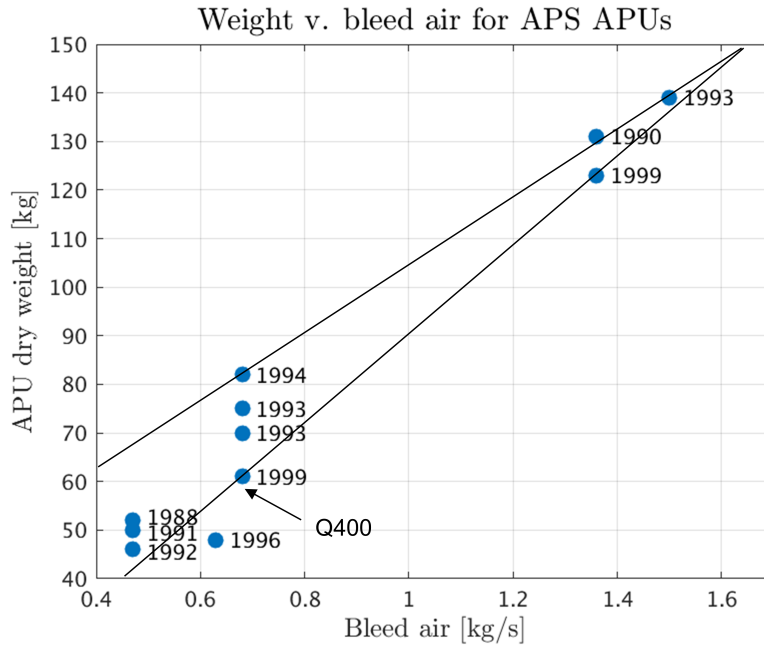


Figure 7: Relationship between bleed air production and APU mass for APS APUs. Year shown is certification year.

Conclusion

The presented modelling framework focuses on a parametric, transient thermal model for the analysis of a solar powered air-conditioning system for aircraft. The associated case study illustrates the potential benefits of the proposed concept of the solar-powered fan. Therefore, the presented work contributes to establish the viability of a solar powered air conditioning system on the conceptual level.

By using a solar powered air recirculation fan, the pull-down loading is reduced resulting in a weight decrease due to the resizing of the APU and the ECS. A case study is presented for the Q400, and the estimated APU weight decrease is presented alongside an estimate for the weight of the SPACS.

As the SPS is capable of providing orders of magnitude more power than is required by the air recirculation fan, a future application could be the usage of a refrigeration system to cool the cabin much faster and cooler than an air recirculation fan. Also, as the SPS is being used to supply auxiliary electrical power whenever the sun is shining, the aircraft fuel burn can be reduced.

Future work includes a more complete modelling framework to improve the assessment of the weight impact. In addition, more work will be done to develop a detailed system integration concept for an auxiliary solar power system for future aircraft.

References

- [1] Climate change. International Air Transport Association. [Online]. Available: <https://www.iata.org/policy/environment/Pages/climate-change.aspx>
- [2] G. Ramirez-Diaz, V. Nadal-Mora, and J. Piechocki, “Descriptive analysis of viability of fuel saving in commercial aircraft through the application of photovoltaic cells,” *Renewable and Sustainable Energy Reviews*, vol. 51, pp. 138–152, 2015. [Online]. Available: <http://dx.doi.org/10.1016/j.rser.2015.06.008>
- [3] S. Liscouët-Hanke, A. Shafiei, L. Lopes, and S. Williamson, “Proof-of-concept analysis of a supplemental solar power system for aircraft,” *Aircraft Engineering and Aerospace Technology*, vol. 9, pp. 1295–1304, 2018. [Online]. Available: <https://doi.org/10.1108/AEAT-08-2017-0189>
- [4] S. Liscouët-Hanke and E. Murugesan, “Conceptual design framework for an aircraft auxiliary solar power system,” *2018 Aviation Technology, Integration, and Operations Conference*, 2018.
- [5] A. Jeyaraj, F. Sanchez, P. Earnest, E. S. Murugesan, and S. Liscouët-Hanke, “Exploring collaborative and multidisciplinary aircraft optimization through the agile academy challenge – a case study for an aircraft auxiliary solar power system,” 2019.
- [6] B. S. Arango, B. R. Hughes, and H. N. Chaudry, “Performance investigation of ground cooling for the airbus A380 in the United Arab Emirates,” *Applied Thermal Engineering*, vol. 36, 2011.
- [7] E. L. Zapparoli and C. R. de Andrade, “Simulation of the aircraft cabin cool-down and warm-up process,” *Instituto Tecnológico de Aeronáutica – Departamento de Energia*, 2003.
- [8] Modelica language. Modelica. [Online]. Available: <https://www.modelica.org/modelicalanguage>
- [9] Dymola. Dassault Systemes. [Online]. Available: <https://www.3ds.com/products-services/catia/products/dymola/>
- [10] BOEING, “Runway pavement surface type descriptions,” MathWorld. [Online]. Available: http://www.boeing.com/assets/pdf/commercial/airports/faqs/boeing_pavement_surface_types.pdf
- [11] D. P. Linares, “Modeling and simulation of an aircraft environmental control system,” Master’s thesis, École Polytechnique de Montréal, 2016.
- [12] Incropera, DeWitt, Bergman, and Lavine, *Fundamentals of heat and mass transfer*. England: Wiley, 2007.
- [13] I. Chakraborty, “Subsystem architecture sizing and analysis for aircraft conceptual design,” Ph.D. dissertation, Georgia Institute of Technology, 2015.
- [14] DAE, “Fans and blowers, 2012 product guide (si units),” catalog. [Online]. Available: http://www.dynamic-air.com/pdf/DAE_Catalog_Volume.1_Intro_B13B_IF_A4.SI.ST.pdf
- [15] *Ventilation and Heating*, Transport Canada Canadian Aviation Regulations Chapter 525.831, 2019. [Online]. Available: <http://www.tc.gc.ca/eng/civilaviation/regserv/cars/part5-standards-525-sub-d-1741.htm#525.831>
- [16] “APU directory,” FlightGlobal, 1997.
- [17] “Auxiliary power units (APU),” Pratt & Whitney Canada. [Online]. Available: <https://www.pwc.ca/en/products-and-services/products/auxiliary-power-units>